ELSEVIER

Journal of Power Sources 93 (2001) 215–223

JOURNAL OF POWER SOURCES

www.elsevier.com/locate/jpowsour

Surface treatment of carbon electrodes by electron beam irradiation

Eishi Endo[a,*], Toru Kihira[b], Shinichiro Yamada[c], Hiroshi Imoto[c], Koji Sekai[c]

[a]*Frontier Science Laboratories, Sony Corporation, Yokohama 240-0036, Japan*
[b]*R&D Patent Department, Sony Corporation, Yokohama 240-0036, Japan*
[c]*CNC Company, Sony Corporation, Yokohama 240-0036, Japan*

Received 5 October 1999; received in revised form 11 August 2000; accepted 1 September 2000

Abstract

An electron beam (EB) was irradiated on carbon anodes of lithium-ion secondary batteries. The discharge capacity was increased by 19 mAh g^{-1} in the mesocarbon microbeads electrode and by 55 mAh g^{-1} in the coffee-bean derived carbon electrode. X-ray photoelectron spectroscopy (XPS) and Raman spectroscopy were used to observe the surface changes which included a reduction in the amount of binder and structural changes in the carbon materials. © 2001 Elsevier Science B.V. All rights reserved.

Keywords: Electron beam irradiation; Carbon electrode; Surface treatment; Lithium-ion battery

1. Introduction

Lithium-ion secondary batteries are widely used for portable electronic devices and the carbon anode is a key component. To achieve better electrode performance, high-capacity carbonaceous anode materials have been developed and ways of modifying the surface of the carbon anodes have also been investigated [1–13]. These surface modifications may require an elevated temperature, vacuum treatment, or a post-treatment procedure to remove solvents or residues or a combination of these, so the process becomes complicated.

Electron beam (EB) irradiation is widely used to modify the surface of organic and inorganic materials [14–20], and the irradiation of the sample in atmospheric pressure is the conventional technique for surface modification of polymer materials [21,22]. This treatment has the following advantages.

1. Gas phase treatment enables uniform surface treatment regardless of the surface roughness.
2. The experimental parameters such as acceleration voltage, current, and conveyer speed are easily controlled.
3. There is no need to remove residues as in liquid phase treatment.
4. It is a conventional treatment and easily scaled up since it does not require heating process, sample chamber evacuation or any other complicated pre- or post-treatment.

In this study, EB irradiation has been used for surface modification of carbon anodes and its effect on the electrode performance is discussed.

2. Experimental

2.1. Electrode preparation

Three kinds of carbon materials were subjected to EB irradiation. The graphitic carbon used was mesocarbon microbeads heated up to 2800°C (MCMB, Osaka Gas Ltd.). Non-graphitizable carbon materials from polyfurfuryl alcohol (PFA-C) [23,24] and from coffee-beans (CB-C) [25] were also used. These carbon materials were first dried under argon atmosphere at 600°C for 90 min. Each of these materials was then mixed with 10% of poly(vinylidene 1,1-difluoride) (PVDF, Aldrich) as binder and pressed with a stainless mesh to form the pellet electrode.

2.2. EB irradiation

Electron beam irradiation of the pellet electrode was carried out using CB250/30/180L electrocurtain processor (Iwasaki Electric Co. Ltd.). The configuration of the appa-

* Corresponding author. Tel.: +81-45-353-6823; fax: +81-45-353-6904.
E-mail address: eishi.endoh@jp.sony.com (E. Endo).

PII: S0378-7753(00)00581-4

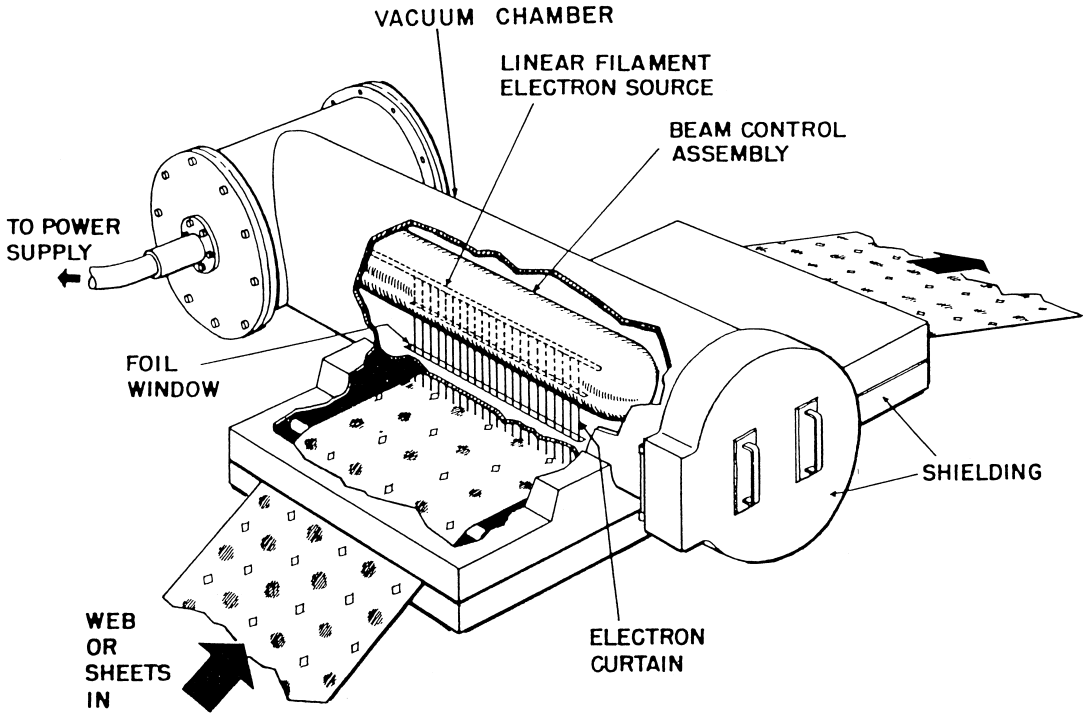

Fig. 1. Schematic diagram of the apparatus for EB irradiation.

ratus is shown in Fig. 1 [21]. Thermoelectrons are generated from the linear filament and accelerated in the vacuum chamber. Then the electron comes out through a titanium foil window into the processing area. The sample was placed in the processing area, which was filled with nitrogen at atmospheric pressure, at an oxygen concentration below 300 ppm.

2.3. Coin-type cell test

The performance of the pellet electrodes was evaluated using a coin-type cell. The test cell was assembled in a 2025 coin-type cell with the electrode pellet, a lithium metal counter electrode, a polypropylene separator and electrolyte solution. The electrolyte solution used was 1 M $LiPF_6$ in 1:1 ethylene carbonate and dimethylcarbonate (EC + DMC) for MCMB cells and in 1:1 propylene carbonate and dimethylcarbonate (PC + DMC) (Tomiyama Pure Chemicals Industry Ltd., electrochemical grade) for non-graphitizable carbon cells. The coin cell was assembled in dry air. Since we are considering application to the anode of lithium-ion batteries, we regarded the lithiation of carbon as charging. Two charge–discharge conditions were used in accordance with the electrode characteristics.

1. Steady-state condition. The cell was charged galvanostatically with a current density of 0.25 mA cm^{-2} to the potential of −20 mV versus Li/Li^+ and discharged to 2000 mV. These are the typical conditions used for the evaluation of graphitic carbon electrodes and were applied to the MCMB cells in this study.
2. Intermittent condition [23,24]. The cell was charged by repetition of the sequence of imposing a current of 0.5 mA cm^{-2} for 1 h followed by 2 h of relaxation. The charge was terminated when the equilibrium potential estimated from the relaxation potential ($t \rightarrow \infty$ in potential versus $t^{-1/2}$ plot) reached 4 mV versus Li/Li^+. Discharging was performed using the same sequence and was terminated when the closed circuit voltage exceeded 1.5 V. We have applied this technique to the evaluation of non-graphitizable carbon cells, PFA-C and CB-C cells in this study.

2.4. Characterization

X-ray diffraction (XRD) patterns were measured using an RINT 2500 V diffractometer (Rigaku Co.) equipped with a Cu Kα radiation source and a diffracted beam monochrometer. X-ray photoelectron spectroscopy (XPS) was performed using an S-probe spectrometer (SII). Raman spectroscopy was performed using an Ar laser (514.5 nm, 40 mW at sample) as the excitation source, a monochrometer (JOBIN YVON T64000), and an LN-cooled 1 in. back-thinned CCD as the detector.

3. Results and discussion

3.1. Electrode performance

The effect of EB irradiation on the electrode performance was evaluated first. Fig. 2 shows the charge–discharge

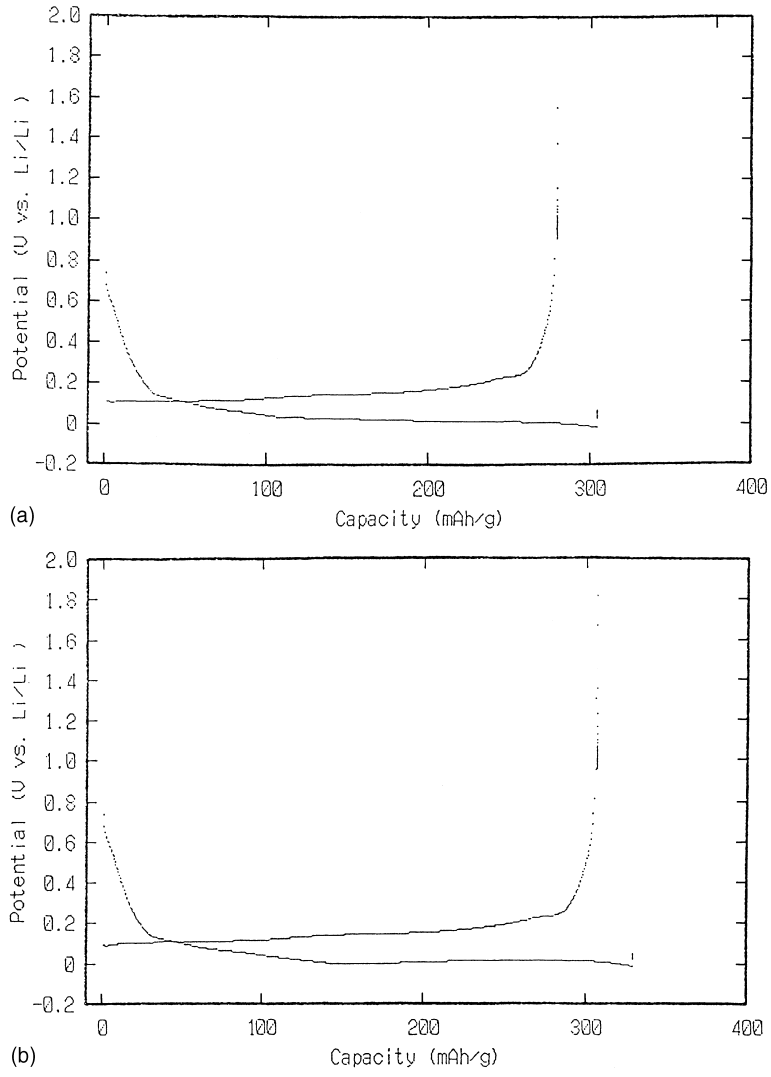

Fig. 2. Charge–discharge curves of MCMB electrodes with (a) 0 and (b) 100 kGy of EB irradiation.

curves of the MCMB electrodes in the first cycle. No significant difference can be seen in the charge–discharge curves, except for the capacity. By EB irradiation, discharge capacity increased from 283 to 302 mAh g^{-1}, while charge capacity increased from 310 to 326 mAh g^{-1}. The discharge capacity was increased by 19 mAh g^{-1} after EB irradiation and the resulted charge–discharge efficiency was also increased slightly.

Fig. 3 shows the cycle performance of the MCMB electrodes. The discharge capacity of the first cycle was smaller than that of the second cycle as the wettability of the separator used was less than optimal, and the cycle performance after the second cycle was improved slightly by EB irradiation. The dose dependence of increased discharge capacity in the second cycle is shown in Fig. 4. Increased capacity was saturated at around 300 kGy.

The electrode performance of the two non-graphitizable carbons was also improved by EB irradiation. The results are shown in Figs. 5 and 6, and in Table 1. While the increase in charge–discharge capacity of the PFA-C electrode was of the order of 10 mAh g^{-1}, a more considerable increase in charge–discharge capacity was observed in the CB-C electrode. The discharge capacity increased 55 mAh g^{-1} after 100 kGy of EB irradiation.

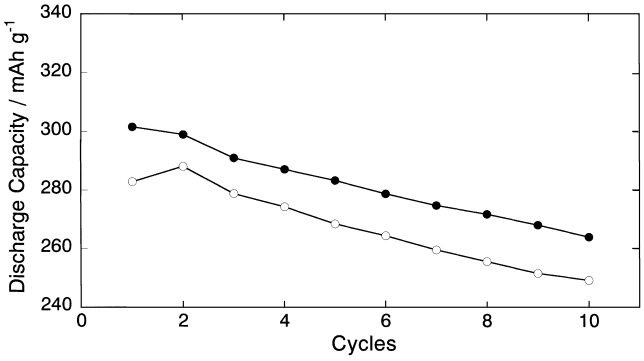

Fig. 3. Discharge capacity of EB-irradiated MCMB electrodes with (○) 0 and (●) 100 kGy of EB irradiation.

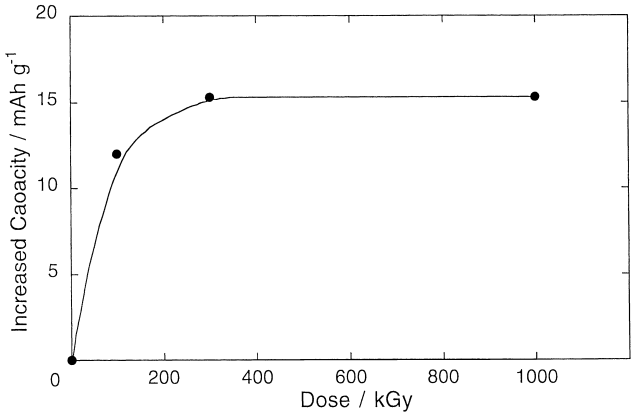

Fig. 4. Dose dependence of increased discharge capacity of MCMB electrodes after EB irradiation.

Thus far, the discharge capacity both of graphitic and of non-graphitizable carbon electrodes was increased by EB irradiation. The intrinsic irreversible capacity of carbon materials was not suppressed, however, the resulted charge–discharge efficiency was slightly increased. The mechanism is discussed in the following section.

3.2. XRD patterns

Fig. 7 shows the XRD patterns of the MCMB electrodes. No characteristic differences were observed between EB-irradiated and non-irradiated electrodes among all the carbon materials we investigated. We conclude that the crystal structure of the bulk carbon materials was not changed by EB irradiation. We then investigated the surface change brought about by EB irradiation.

3.3. X-ray photoelectron spectra

The surface structure of the carbon electrodes was characterized using XPS. Fig. 8a shows the C 1 s spectrum of the MCMB electrodes. Photoelectron peaks at 284.5, 286.3 and

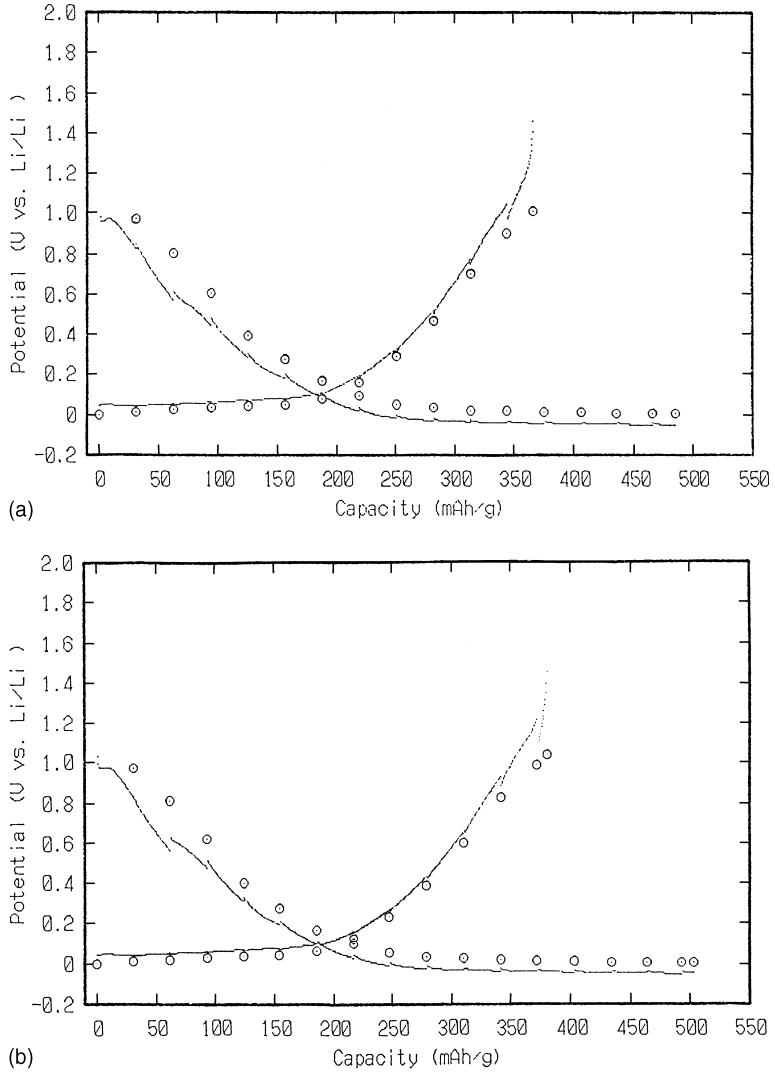

Fig. 5. Charge–discharge curves of PFA-C electrodes with (a) 0 and (b) 100 kGy of EB irradiation.

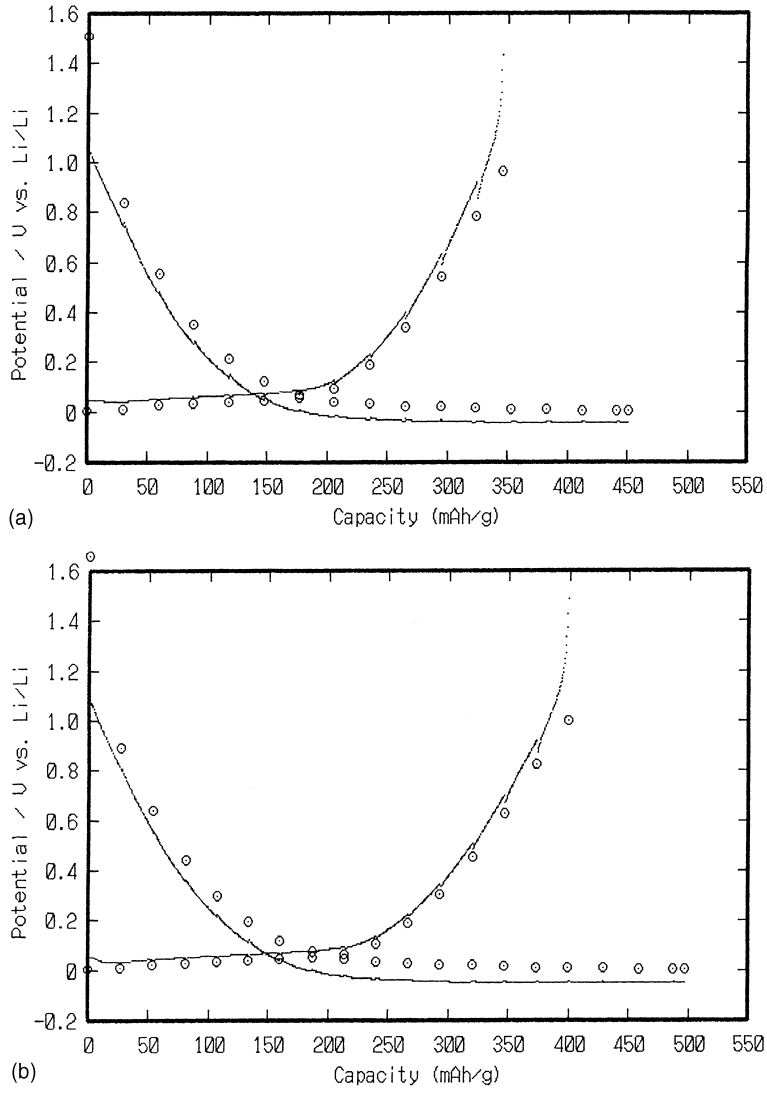

Fig. 6. Charge–discharge curves of CB-C electrodes with (a) 0 and (b) 100 kGy of EB irradiation.

291 eV were observed before EB irradiation, and the latter two peaks were decreased by 100 kGy of irradiation. These three peaks are attributed to C–C bonds of graphite, CH_2 and CF_2 of PVDF, respectively. It appears that a portion of the binder components are eliminated by EB irradiation.

It has been reported that fluorine in polymer surfaces is eliminated by EB irradiation [26]. Further, structural change of vinyl polymers brought about by EB irradiation has been reported by Dong and Bell [27]. They reported cross-linking results from EB irradiation when the structure of a vinyl polymer is such that each carbon atom of the main chain is bound to at least one hydrogen atom. Alternatively, if a tetrasubstituted carbon atom is present in the monomer unit, the polymer is degraded by EB irradiation. This supposition is supported by the fact that the carbon bond in the main chain can be weakened by the presence of the tetrasubstituted carbon atom, since they cause a strain in the molecule by the steric repulsion effect. PVDF, the present binder, contains tetrasubstituted carbon atoms. So the elimination of PVDF binder by EB irradiation is consistent with Dong's

Table 1
Electrode performance of EB-irradiated non-graphitizable carbon electrodes

Electrode	Dose (kGy)	Discharge capacity (mAh^{-1})	Charge capacity (mAh^{-1})	Efficiency (%)
PFA-C	100	384.9	503.7	76.4
	0	377.5	495.8	76.1
CB-C	100	401.0	497.0	80.7
	0	346.0	456.0	75.9

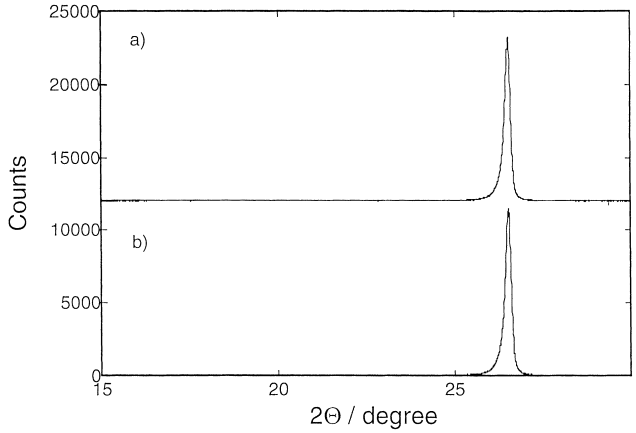

Fig. 7. XRD patterns of MCMB electrodes with (a) 0 and (b) 100 kGy of EB irradiation.

supposition. It is naturally accepted that the binder content affects the electrode performance [28], in the bulk and at the electrolyte interface.

The other minor change observed using XPS is the increase of oxygen on the MCMB electrode surface with EB irradiation, as shown in Fig. 8b. An O 1 s photoelectron peak was observed at 533.2 eV after EB irradiation. This peak is attributed to the OH group connected to a benzene ring, so it should be the result of the reaction of graphitic carbon with water in the atmosphere. However, the oxygen content was of the order of 1% at the electrode surface, so it should not significantly effect the electrode performance.

The same phenomena were observed in non-graphitizable carbon electrodes. Fig. 9 shows the XPS spectra of PFA-C electrodes. Peaks attributed to the binder decreased and the oxygen content increased slightly with EB irradiation. Accordingly, the binder on the electrode surface was reduced by EB irradiation and this affects electrode performance. EB irradiation, however, could also affect the structure of the carbon materials themselves.

3.4. Raman spectra

Raman spectroscopy is useful for characterizing the surface structure of carbon materials to a depth of several hundreds of nanometers. In this study, the structural changes of the carbon electrode surface after EB irradiation were investigated. Fig. 10 shows the Raman spectra of the MCMB electrodes. The observed spectra combine four peaks characteristic of defined carbon structures. The strong band at 1580 cm^{-1} indicates an E_{2g2} vibration mode in the graphitic region of carbon materials (G-band) and the bands at 1350 and 1620 cm^{-1} show an A_{1g} mode arising from the (dis-

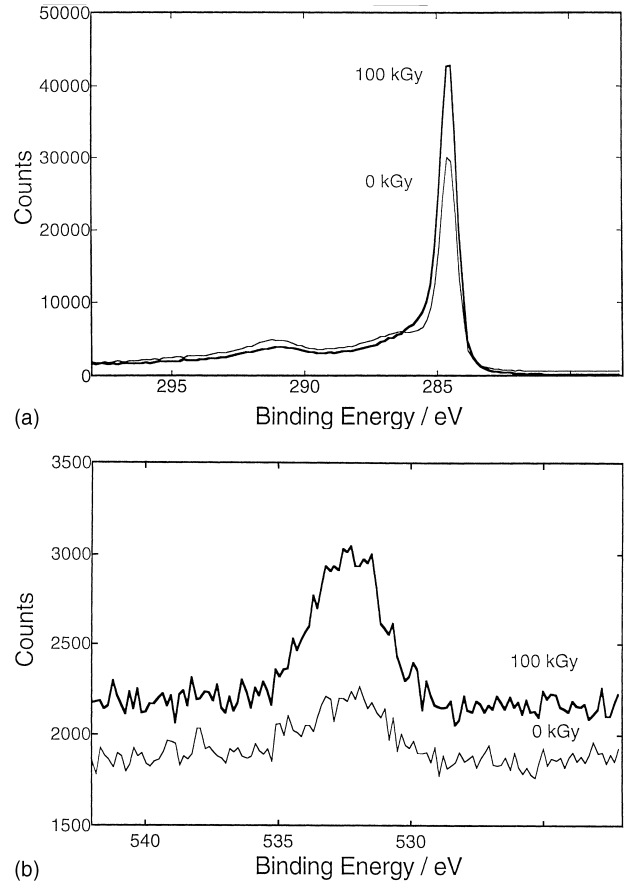

Fig. 8. (a) C 1 s and (b) O 1 s photoelectron spectra for the MCMB electrodes.

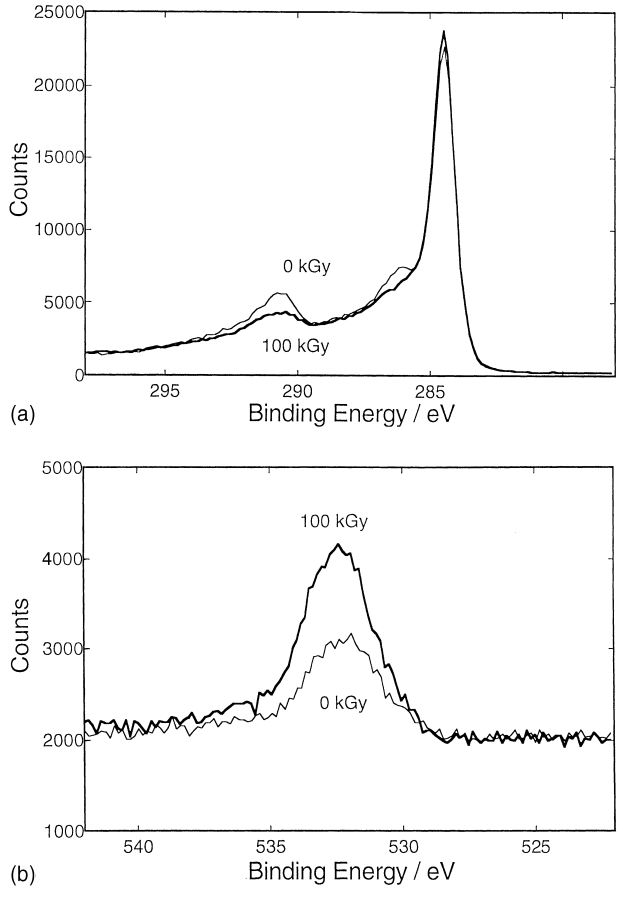

Fig. 9. (a) C 1 s and (b) O 1 s photoelectron spectra for the PFA-C electrodes.

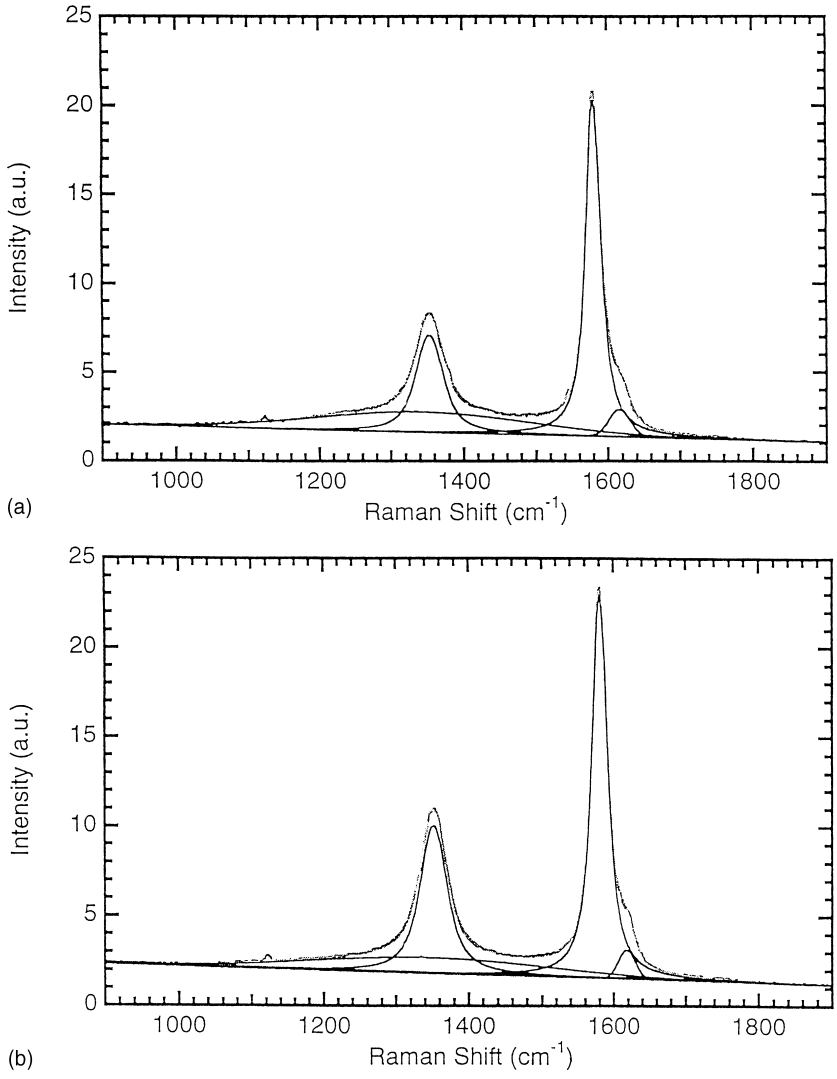

Fig. 10. Raman spectra of MCMB electrodes with (a) 0 and (b) 100 kGy of EB irradiation.

ordered) turbostratic structure in carbon (D-band) [29,30]. The broad Gaussian-shape band at around 1300 cm^{-1} is from an amorphous (non-periodical) carbon structure. In the MCMB electrode, the peak of the graphitic structure is narrow and high, suggesting the development of the graphitic structure in MCMB. However, peaks of the turbostratic structure and of the amorphous structure are also observed.

After EB irradiation, the area of the peaks at 1350 and 1580 cm^{-1} increased, while that of the broad peak at 1300 cm^{-1} decreased. This means that the amorphous component decreased with EB irradiation, and as a result, the turbostratic and graphitic components were enhanced. The possibilities for structural change are either changing the amorphous component into some ordered structure or simply eliminating the amorphous component by EB irradiation. In order to carry out a detailed analysis of the structural change, the parameter R was calculated and is shown in Fig. 11. The ratio of D-band (1350 cm^{-1}) to G-band (1580 cm^{-1}) intensities, R (I_D/I_G) [29,30] expresses the degree of surface disordering of the graphite powder. The R value of the MCMB electrode was increased by EB irradiation, suggesting a greater increase in the turbostratic component versus the graphitic component. The amorphous

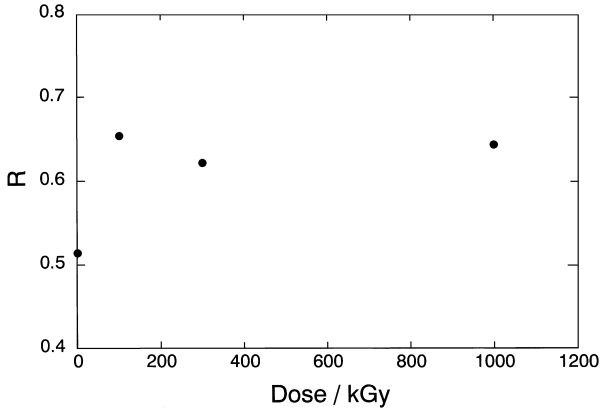

Fig. 11. Dose dependence of R value of EB-irradiated MCMB electrodes.

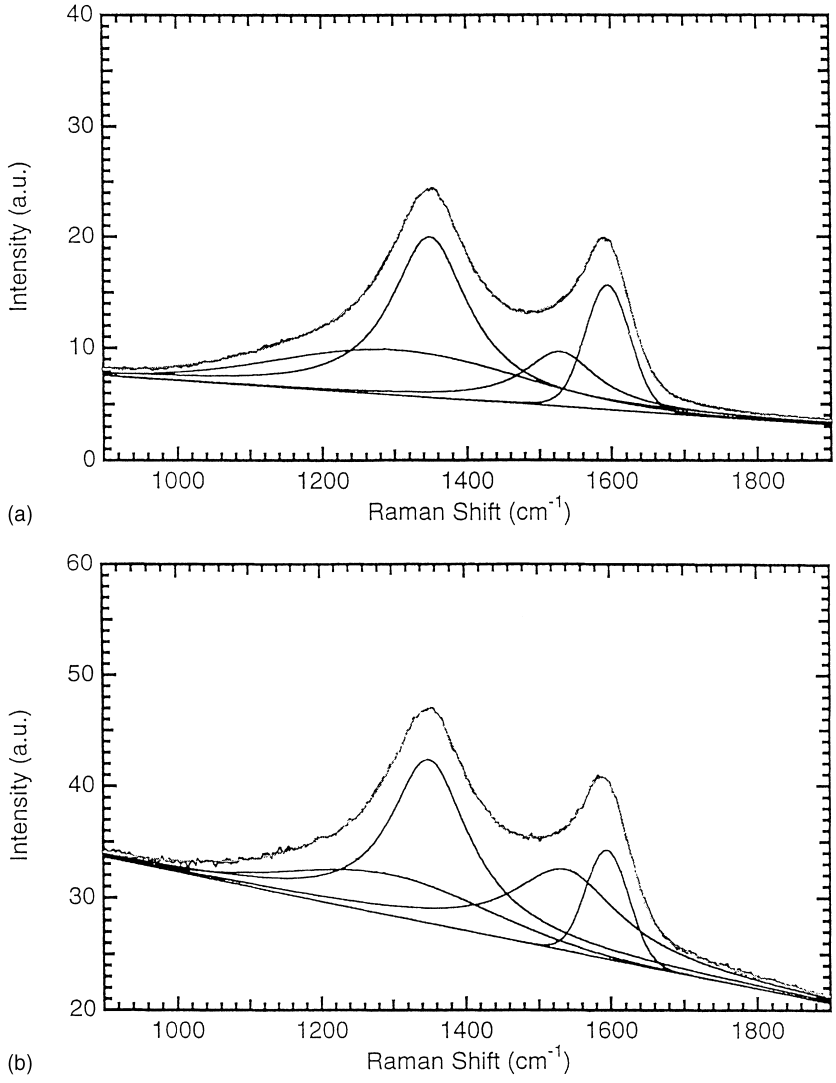

Fig. 12. Raman spectra of PFA-C electrodes after (a) 0 and (b) 100 kGy of EB irradiation.

component exists primarily at the grain boundary and can be changed into turbostratic structure by EB irradiation. The turbostratic component contributes to additional electrode performance.

The Raman spectra of non-graphitizable carbon was also changed by EB irradiation, as is shown in Fig. 12. The spectra can be separated into the four characteristic bands described above, and the same structural changes were observed: (1) the amorphous components were decreased and (2) the ordered structural components were increased by EB irradiation. Unfortunately, intense fluorescence and extremely broad peaks make it impossible to completely eliminate background scattering and prevents a more detailed discussion of the data.

One possible explanation of the increased capacity of CB-C over PFA-C is binder-carbon particle interaction. The extent of this interaction depends on particle size, shape and the type of carbon material. Another possibility is the differences in the structural changes of the carbon materials brought about by EB irradiation, although this has not yet been confirmed.

4. Conclusion

The discharge capacity of all carbon electrodes is increased by EB irradiation. The type of change brought about depends on the carbon electrode. EB irradiation eliminates some binder components from the electrode surface and also change the surface structure of the carbon materials.

Acknowledgements

We gratefully thank Iwasaki Electric Co. Ltd. and Energy Sciences Inc. for their kind cooperation with EB irradiation and discussions. We also thank Dr. M. Ata, A. Kita, Y.

Gonno, K. Satori, and K. Kitamura for their helpful discussions and technical assistance. Sony Corporation assisted in meeting the publication costs of this article.

References

[1] M. Kikuchi, Y. Ikezawa, T. Takamura, J. Electroanal. Chem. 196 (1995) 451.
[2] T. Takamura, H. Awano, T. Ura, K. Sumiya, J. Power Sources 68 (1997) 114.
[3] J.S. Xue, J.R. Dahn, J. Electrochem. Soc. 142 (1995) 3668.
[4] C. Liebenow, M.W. Wagner, K. Luehder, P. Lobitz, J.O. Besenhard, J. Power Sources 54 (1995) 369.
[5] K. Tatsumi, K. Zaghib, H. Abe, S. Higuchi, T. Ohsaki, Y. Sawada, J. Power Sources 54 (1995) 425.
[6] E. Peled, C. Menachem, D. Bar-Tow, A. Melman, J. Electrochem. Soc. 143 (1996) L4.
[7] C. Menachem, D. Golodnitsky, E. Peled, in: C.F. Holmes, A.R. Landgrebe (Eds.), Proceedings of the Symposium on Batteries for Portable Applications and Electric Vehicles, PV 97-18, The Electrochemical Society Proceedings Series, Pennington, NJ, 1997, p. 95.
[8] C. Meanchem, Y. Wang, J. Flowers, E. Peled, S.G. Greenbaum, J. Power Sources 76 (1998) 180.
[9] Y. Ein-Eli, V.R. Koch, J. Electrochem. Soc. 144 (1997) 2968.
[10] T.D. Tran, L.C. Murguia, X. Song, K. Kinoshita, in: C.F. Holmes, A.R. Landgrebe (Eds.), Proceedings of the Symposium on Batteries for Portable Applications and Electric Vehicles, PV 97-18, The Electrochemical Society Proceedings Series, Pennington, NJ, 1997, p. 82.
[11] T. Nakajima, M. Koh, M. Takashima, Electrochim. Acta 43 (1998) 883.
[12] T. Nakajima, M. Koh, R.N. Singh, M. Shimada, Electrochim. Acta 44 (1999) 2879.
[13] F. Joho, P. Novak, O. Haas, A. Monnier, F. Fischer, Mol. Cryst. Liq. Cryst. 310 (1998) 383.
[14] T. Uchida, H. Kaneko, Y. Yasuoka, K. Gamo, S. Namba, Jpn. J. Appl. Phys. 34 (1995) 2049.
[15] F. Yoshii, K. Makuuchi, S. Kikukawa, T. Tanaka, J. Saitoh, K. Koyama, J. Appl. Polym. Sci. 60 (1996) 617.
[16] O.N. Tretinnikov, S. Ogata, Y. Ikada, Polymer 39 (1998) 6115.
[17] I. Lieberwirth, F. Katzenberg, J. Petermann, Adv. Mater. 10 (1998) 997.
[18] T. Ohi, O. Konno, J. Vac. Sci. Technol. A12 (1994) 3186.
[19] D. Grozea, E. Landree, L.D. Marks, Appl. Phys. Lett. 71 (1997) 2301.
[20] K. Kawasaki, K. Tsutsui, Appl. Surf. Sci. 117/118 (1997) 753.
[21] E.P. Tripp III, Proc. Water-Borne Higher-Solids Coat. Symp. 14 (1987) 46.
[22] J.E. Wyman, I.J. Rangwalla, S.V. Nablo, Polym. Pater. Sci. Eng. 60 (1989) 463.
[23] H. Imoto, A. Omaru, H. Azuma, Y. Nishi, in: S. Surampudi, V. Koch (Eds.), Proceedings of the 4th International Symposium on Lithium Batteries, PV 93-24, The Electrochemical Society Proceedings Series, Pennington, NJ, 1993, p. 9.
[24] H. Imoto, M. Nagamine, Y. Nishi, in: S.A. Megahed (Ed.), Rechargeable Lithium and Lithium Ion (RCT) Batteries, PV 94-28, The Electrochemical Society Proceedings Series, Pennington, NJ, 1994, p. 43.
[25] S. Yamada, H. Imoto, K. Sekai, M. Nagamine, Extended Abstracts of 191st Electrochemical Society Meeting, Montreal, Canada, 4–9 May 1997, p. 85.
[26] Y.Y. Maruo, S. Sasaki, T. Tamamura, Jpn. J. Appl. Phys. 35 (1996) L523.
[27] H. Dong, T. Bell, Surf. Coat. Technol. 111 (1999) 29.
[28] G. Li, R. Xue, L. Chen, Solid State Ionics 90 (1996) 221.
[29] T. Tunistra, J.L. Koenig, J. Chem. Phys. 53 (1970) 1126.
[30] D.S. Knight, W.B. White, J. Mater. Res. 4 (1989) 385.